

## Functionalization of Silica Surface by Tetrahydroxyprophyrin via Si–O Linkages

Nagisa Minamijima, Nao Furuta, Shintaro Wakunami, and Tadashi Mizutani\*

Department of Molecular Chemistry and Biochemistry, Faculty of Science and Engineering, Doshisha University, Tatara-miyakodani, Kyotanabe, Kyoto 610-0321

Received November 15, 2010; E-mail: tmizutan@mail.doshisha.ac.jp

To construct an interface between a  $\pi$ -conjugated organic molecule and an inorganic/metal surface, 5,10,15,20-tetrakis[4-(5-hydroxypentyl-oxy)phenyl]porphyrin was chemisorbed on silica gel by refluxing in pyridine. Thermogravimetric analysis confirmed that 1.5–6.3 mg tetrahydroxyprophyrin was adsorbed on 50 mg of silica gel. To functionalize the surface of a silicate glass plate with the porphyrin, a spin-coated film of the porphyrin on the glass plate was heated at 80–296 °C, followed by sonication in pyridine to remove the unreacted porphyrin. Heating above 130 °C gave a monolayer film. The reaction proceeds between two solid phases since the melting point of the porphyrin was 293 °C. The threshold temperature for the reaction to proceed was 90, 160, and 250 °C for 5,10,15,20-tetrakis[4-(5-hydroxypentyl-oxy)phenyl]porphyrin, 5,10,15,20-tetrakis[4-(5-acetoxypentyl-oxy)phenyl]porphyrin, and 5,10,15,20-tetrakis(4-hexyloxy-phenyl)porphyrin, respectively. The different reactivities of the alcohol, ester, and other functional groups could be used to construct highly sophisticated organic–inorganic surfaces.

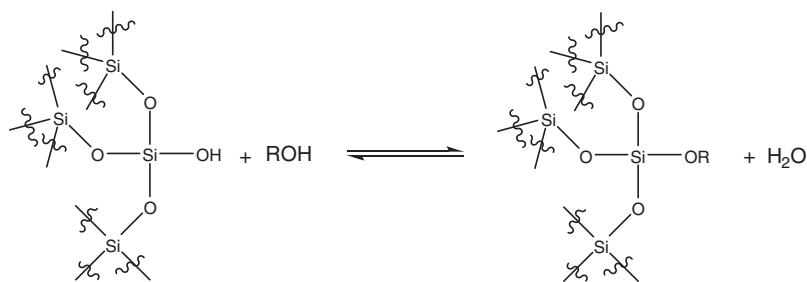
For the development of electronic devices by use of semiconducting organic molecules, control of the interfacial structure between the organic active layer and metallic/inorganic electrodes is important, particularly for nanoelectronics fabrication.<sup>1–4</sup> For instance, electric conducting polymers have been used to cover an electrode to have good communication between the electrode and the active layer of electronic devices.<sup>5–7</sup> The structures of the interfaces have been characterized by spectroscopic<sup>8–11</sup> and microscopic techniques.<sup>12,13</sup> Ishii and co-workers have studied the UV photoemission spectra of several porphyrin derivatives deposited on Mg, Ag, and Au, and have revealed the electronic structures of porphyrins and the interface between the porphyrins and the metals.<sup>14,15</sup>

There have been several approaches to construct an interface between organic molecules and metal surfaces. Reaction of thiols with Au was used to construct metal–molecule–metal junctions.<sup>16</sup> Zaera and co-workers have reported the preparation of a porphyrin monolayer on Si(100) via Si–C bonds, and revealed that the electron-transfer rate between the porphyrin and silicon depended on the linker structures.<sup>17</sup> It is well-known that the oxide layer forms on the surface of metallic Si under ambient conditions.<sup>11</sup> Our strategy<sup>18–20</sup> is to use the thin oxide layer on the surface of silicon<sup>21–25</sup> to attach  $\pi$ -conjugated molecules covalently where the oxide layer can be formed under controlled conditions. The reaction is a reverse of the sol–gel process, in which the organic groups are eliminated from the inorganic particle as an alcohol.<sup>26,27</sup> We envisioned that covalent attachment of the organic molecules could result in a stable and more ordered interface than simple deposition of organic layer on the metal surface.<sup>28</sup> We employed porphyrin with four reactive groups to attach to the SiO<sub>2</sub> surface through multiple covalent bonds. Mirkin,

Hoffman, and co-workers have demonstrated that multivalency of the organic molecule can regulate the orientation of discotic molecules to the metal surface.<sup>29</sup> The object of this study is to establish a procedure to covalently bind a porphyrin molecule onto the surface of silicon oxide.<sup>30,31</sup> We have studied the reaction between tetrahydroxyprophyrin and silica to functionalize the silica surface with porphyrin via silicate ester linkages, and have characterized the resulting porphyrin layer on the SiO<sub>2</sub> surface.

Reaction of alcohols with silica gel has been the subject of active investigations.<sup>32,33</sup> The alcohols employed have been limited to relatively simple ones such as ethanol, butanol, and octanol.<sup>34,35</sup> The reaction shown in Scheme 1 is a reversible reaction, and proceeds in both directions depending on the reaction conditions. The esterification proceeds by a nucleophilic attack of alcohol oxygen on silicon, while hydrolysis occurs by a nucleophilic attack of water on silicon, i.e., via silyl–oxygen fission.<sup>36</sup> Ballard and co-workers have reported<sup>34</sup> that the esterification reaction is endothermic, and proceeds at elevated temperatures under anhydrous conditions. The reaction can also be performed by continuous removal of water by azeotropic distillation.<sup>37</sup> Recently, the structure of alcohols and the stability of the resulting silicic acid ester was studied, and branched alcohols and polyols such as poly(vinyl alcohol) formed a more stable ester than did a simple alcohol.<sup>38</sup>

Other approaches to the preparation of porphyrin–silica hybrid materials are to use trialkoxysilane as a coupling reagent. Battioni and co-workers have reported<sup>39</sup> that polycondensation of triethoxypropylamino-substituted iron porphyrin or cocondensation of it with tetraethoxysilane to prepare a new catalyst for alkene epoxidation or alkane hydroxylation. Compared to using silane coupling reagents, advantages of



Scheme 1.

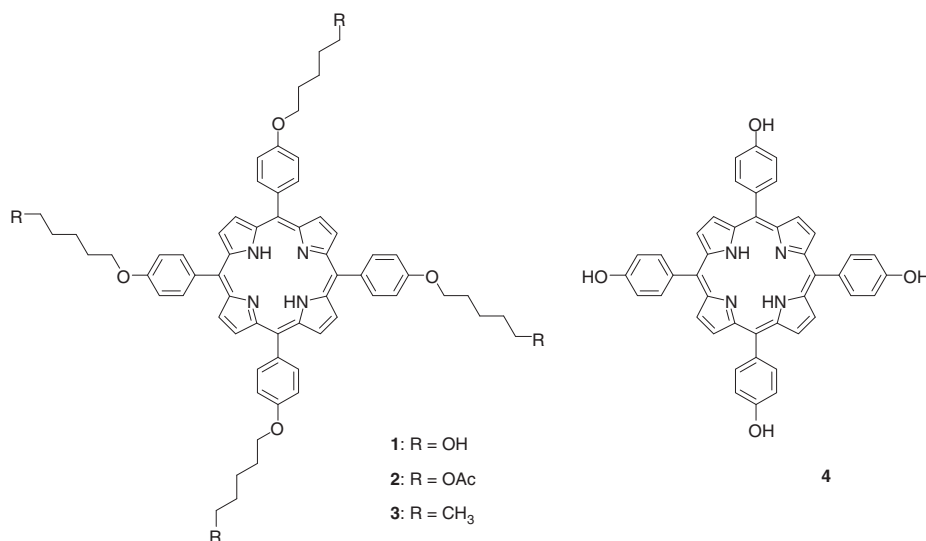


Chart 1. Porphyrin derivatives 1, 2, 3, and 4.

using alcohol to modify silica gel and silicate glass are twofold: (1) alcohols are more stable than silicate esters, which are susceptible to hydrolysis, and the preparation and purification of alcohols is more facile than silicate esters, and (2) reaction of trialkoxysilane with silica gel gives the self-condensation products of trialkoxysilane itself in a side reaction in the presence of water, and once they are formed, their removal is difficult. Alcohols do not give such by-products under the condensation reaction conditions.

We report here that the tetrahydroxyporphyrin was adsorbed on silica gel and silicate glass either in pyridine or by use of a solid–solid reaction. The resulting porphyrin on silicate glass was stable in various solvents, and potentially useful as a substrate for further chemical modifications. In the solid–solid reaction between the tetrahydroxyporphyrin and silicate glass, the porphyrin forms a J-aggregate, as the coverage with the porphyrin was higher. The alcohol, ester, and ether functional groups exhibited different reactivity in the reaction with silicate glass, which could be used to build an organic interface on silicate glass in a more sophisticated fashion.

### Experimental

**Instruments.** Thermogravimetric (TG) analysis and differential scanning calorimetry (DSC) were performed using a Shimadzu DTG-60A and DSC-60, respectively. A hot stage Mettler-Toledo FP82HT was used for heat treatment of the spin-coated films. UV–visible spectra were obtained with a Perkin-Elmer Lambda 950 spectrophotometer or with

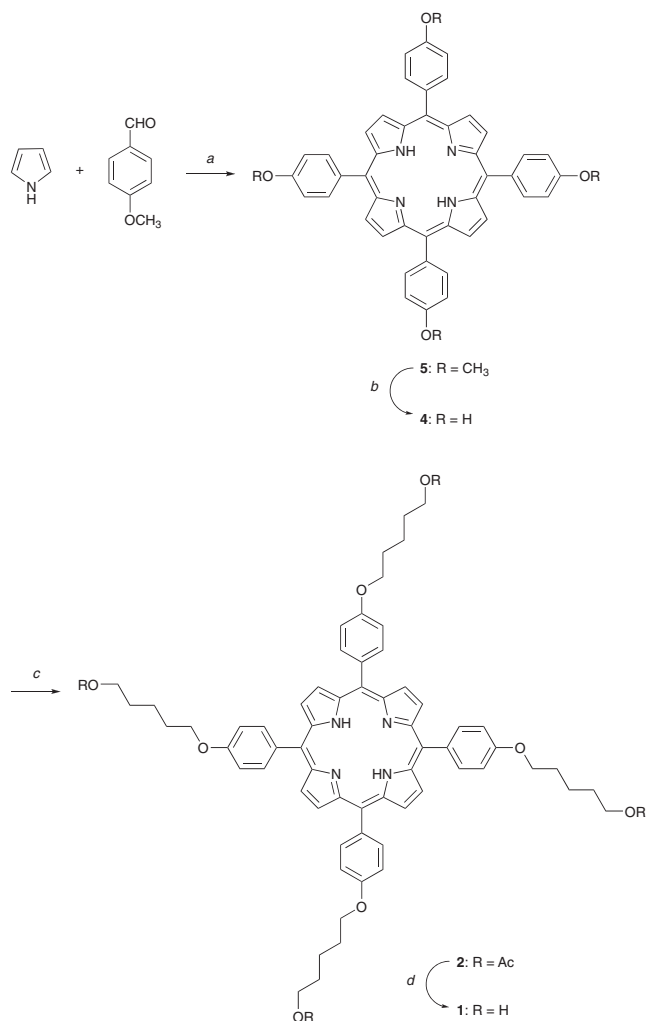
a Shimadzu Multispec-1500 spectrophotometer. Silica gel, CARiACT Q-6, was purchased from Fuji Silysia Chemical Ltd. It had a specific surface area of 451 m<sup>2</sup> g<sup>-1</sup>. 18 mm × 18 mm Borosilicate cover glass plates, Matsunami Trophy, were used for reactions with porphyrins.

**Reaction of 1 with Silica Gel.** Porphyrin 1 (9 mg, Chart 1) was dissolved in pyridine (0.5 mL) and 50 mg CARiACT Q-6 was added. The suspension was heated at 110 °C for 1 h and the pyridine was evaporated over a period of 2 h to dryness. The silica gel was collected by suction filtration, and was washed in pyridine in a bath sonicator. The red silica gel was collected by suction filtration and dried in vacuo. The silica gel was subjected to TG-DTA.

**Reaction of 1 with Silicate Glass.** A glass plate was washed with a solution of H<sub>2</sub>SO<sub>4</sub>:H<sub>2</sub>O<sub>2</sub> (3/1) for 1 h at 80 °C, with water for 30 s, and then with water for 10 min in a bath sonicator. The glass plate was then dried with N<sub>2</sub> gas. A pyridine solution of 1 (60 μL, 4.2 mM) was spin-coated on the silicate glass plate at 3000 rpm for 60 s. The porphyrin film on the glass was heated at 80–296 °C for 10 min using a hot stage. The silicate glass was then washed in pyridine in a bath sonicator to remove unreacted porphyrin. The resultant glass adsorbing porphyrin was analyzed by UV–visible spectroscopy.

### Results and Discussion

**Preparation of Tetrahydroxyporphyrin.** We prepared a porphyrin bearing four hydroxy groups in the periphery according to Scheme 2. Four hydroxy groups were attached



**Scheme 2.** Synthesis of tetrahydroxyporphyrin **1**. Reagents and conditions: *a* propionic acid, reflux; *b* pyridinium hydrochloride, 22 h, reflux; *c*  $\text{Br}(\text{CH}_2)_5\text{OCOCH}_3$ ,  $\text{K}_2\text{CO}_3$ , 18-crown-6, 60 °C, 2 h; *d*  $\text{NaOCH}_3$ , THF, reflux 3 h.

to the porphyrin core through a flexible spacer of the pentamethylene groups. Porphyrin **1** was characterized by  $^1\text{H}$ NMR, mass spectroscopy, and combustion analysis. Porphyrin **1** was soluble in pyridine, while it was sparingly soluble in chloroform and dichloromethane. For control experiments, porphyrins having ester, ether, and phenolic OH functional groups **2**, **3**, and **4** were employed (Chart 1).

**Reaction of Porphyrin 1 with Silica Gel.** A reaction of **1** with silica gel in dry pyridine gave the **1**-silica hybrid. It was deep red as shown in Figure 1. The amount of adsorbed porphyrin was determined by TG analysis. The typical TG curves of the **1**-silica hybrid, the silica gel, and **1** are shown in Figure 2. A sample of the **1**-silica hybrid showed a weight loss in the temperature range 40–220 °C and another weight loss in the temperature range 380–620 °C. A sample of silica alone showed a weight loss in the temperature range 40–130 °C and another weight loss in the temperature range 360–650 °C. We ascribe the first weight loss of both **1**-silica and silica alone to the loss of adsorbed water. The second weight loss of silica alone should then be due to the condensation reaction of Si–OH to Si–O–Si. We observed an exothermic reaction of **1**-silica in

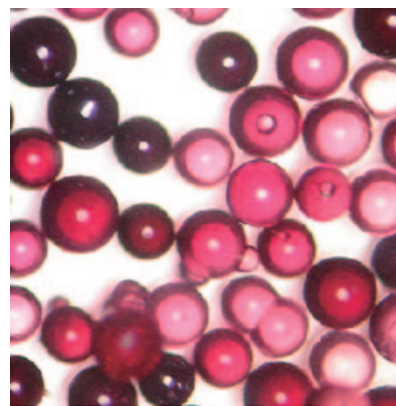


**Figure 1.** Silica gel, CARIACT Q-6, functionalized with **1**.

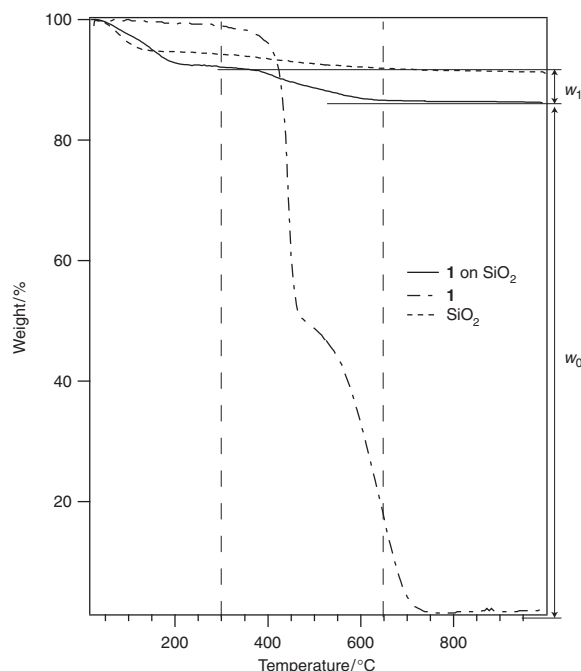


**Figure 2.** TG traces of **1** adsorbed on the silica gel, **1**, and the silica gel. The sample was heated at a rate of 15 °C  $\text{min}^{-1}$  in air. Porphyrin **1** (9 mg) was allowed to react with CARIACT (50 mg) at 110 °C in pyridine (0.5 mL). Evaporation of the pyridine, addition of another portion of pyridine, and heating at 110 °C was repeated three times.

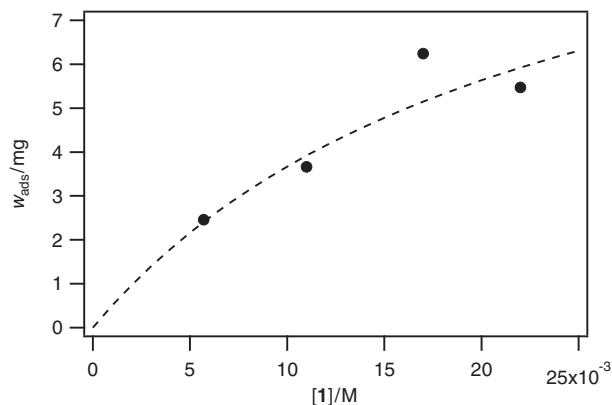
the temperature range 340–650 °C by the use of DTA measurements (data not shown). Therefore the second weight loss of **1**-silica was ascribed to the combustion of **1**. The sample of **1**-silica after heat treatment at 650 °C was colorless, showing that all organic components were eliminated. Thus, we determined the amounts of **1** adsorbed onto silica based on the second weight loss.

The calculation of the adsorbed amount of porphyrin was performed as described in Electronic Supporting Information (ESI). The amounts of the porphyrin adsorbed onto the silica,  $w_{\text{ads}}$ , calculated according to eq 2 (ESI) are listed in Table 1. The values of  $w_{\text{ads}}$  ranged from 0.4 to 6.3 mg/50 mg of  $\text{SiO}_2$  depending on the reaction conditions. As shown in Figure 3, the values of  $w_{\text{ads}}$  increased as the initial concentration of **1** was

**Table 1.** Amounts of Adsorbed **1** on Silica Gel, CARiACT Q-6 (50 mg) in the Reaction in Pyridine

Run	<b>1</b> in the initial solution, [ <b>1</b> ]	Pyridine /mL	Temperature /°C	Time /h	<b>1</b> adsorbed, $w_{\text{ads}}/\text{mg}$
1	4.9 mg, $2.5 \times 10^{-2} \text{ M}$	0.4	110	4	2.8
2	3.0 mg, $9.4 \times 10^{-4} \text{ M}$	3	110	2.5	1.5
3	9.0 mg, $2.8 \times 10^{-3} \text{ M}$	3	110	2.5	2.2
4	3.0 mg, $5.7 \times 10^{-3} \text{ M}$	0.5	110	0.5	0.4
5	3.0 mg, $5.7 \times 10^{-3} \text{ M}$	0.5	110	2.0	2.2
6	3.0 mg, $5.7 \times 10^{-3} \text{ M}$	0.5	110	$2.0 \times 3^{\text{a}}$	2.5
7	6.0 mg, $1.1 \times 10^{-2} \text{ M}$	0.5	110	$2.0 \times 3^{\text{a}}$	3.7
8	9.0 mg, $1.7 \times 10^{-2} \text{ M}$	0.5	110	$2.0 \times 3^{\text{a}}$	6.3
9	12.0 mg, $2.3 \times 10^{-2} \text{ M}$	0.5	110	$2.0 \times 3^{\text{a}}$	4.7
10	3.0 mg, $5.7 \times 10^{-3} \text{ M}$	0.5	rt	2.0	—

a) A cycle of heating at the designated temperature, evaporation of the solvent, and addition of pyridine was repeated three times.

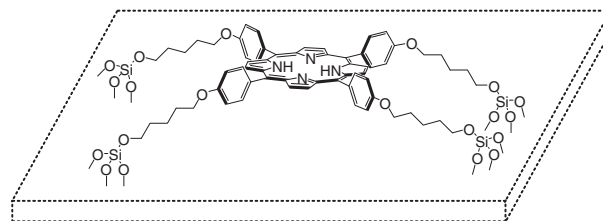
**Figure 3.** Plot of adsorbed **1** onto 50 mg of CARiACT against the concentration of **1** in pyridine. Data taken from Runs 6–9 in Table 1. The dotted line is drawn on the basis of the Langmuir isotherm:  $w_{\text{ads}} = w_{\text{max}}a[\mathbf{1}]/(1 + a[\mathbf{1}])$ .

increased. The amounts of adsorbed **1** were higher when solvent evaporation and addition were repeated, indicating that water removal during evaporation drove the equilibrium shown in Scheme 1 to the silicate ester formation (Run 5 and Run 6 in Table 1).

Adsorption of **1** was also carried out in a solvent-free system: **1** (9 mg) was dissolved in a minimum amount of pyridine, and silica gel (50 mg) was added. The pyridine was evaporated in vacuo, and the resulting powder was heated at 50–296 °C for 2–10 min. The amounts of adsorbed **1** was determined by TG and are listed in Table 2. Compared to the reaction in pyridine, similar amounts of **1** was adsorbed in a much shorter reaction period.

**Table 2.** Amounts of Adsorbed **1** on Silica Gel (50 mg) in the Solvent-Free Reaction

Run	<b>1</b> /mg	Temperature /°C	Time /min	<b>1</b> adsorbed, $w_{\text{ads}}/\text{mg}$
1	9.0	50	10	0.4
2	9.0	110	10	1.2
3	9.0	130	10	1.4
4	9.0	296	2	6.0

**Figure 4.** Schematic representation of **1** adsorbed onto silica surface.

Since the BET surface area of CARiACT Q-6 is  $451 \text{ m}^2 \text{ g}^{-1}$ , 50 mg of CARiACT has a surface area of  $22.5 \text{ m}^2$ . The geometry of **1** with all *trans*-configuration of the methylene chains optimized using ab initio calculations at the B3LYP/6-31G(d) level showed that the distance between two *cis*-oxygen is  $2.31 \pm 0.014 \text{ nm}$ . If we assume that **1** is a  $2.3\text{-nm}$ -square, 3 mg of **1** occupies the area of  $9.3 \text{ m}^2$ , assuming that the porphyrin plane is parallel to the silica surface (Figure 4). The calculation shows that ca. 41% of the BET surface area is occupied by the adsorbed porphyrin. The BET surface area is obtained by use of adsorption of dinitrogen, which is a much smaller molecule than porphyrin. Therefore the surface available for dinitrogen to be bound is not necessarily available for **1** to be bound, depending on the surface roughness of the silica. Therefore the discrepancy between the BET surface area and the surface area covered by **1** may be caused by the difference in molecular size between **1** and  $\text{N}_2$ . The surface coverage of simple alcohols are reported in literature.<sup>40</sup> The value of  $3.22 \mu\text{mol m}^{-2}$  reported for 1-butanol is larger than  $0.16 \mu\text{mol m}^{-2}$  observed for **1**. The difference may be ascribed to the larger size of **1** and also to the polyvalency of **1**, where the molecular orientation should be more restricted.

To evaluate the stability of the **1**- $\text{SiO}_2$  hybrid and to confirm that the porphyrin structure was intact other than silicate ester formation during the reaction with silica, the hybrid (Run 8, Table 1) was added to boiling water and heated at reflux for 2 h. The hybrid was collected by filtration and washed with pyridine. The pyridine turned red, thus showing that some of **1** were liberated due to hydrolysis of the silicic ester linkages. The **1**-silica hybrid after washed with pyridine was still red, and the TG analysis revealed that about 30% of **1** remained on the silica surface. The UV-visible spectrum of the recovered porphyrin showed that the Soret band and the four Q-band appeared at the same wavelengths as original **1**, showing that the porphyrin was not metallated and the structure was unaltered when adsorbed onto the silica surface. Interestingly, when the hybrid obtained in the solvent-free reaction (Run 4, Table 2) was similarly boiled in water for 2 h, 89% of **1**

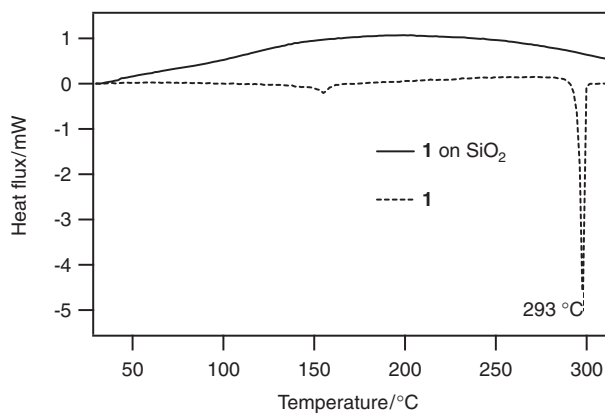


**Figure 5.** The DSC traces of **1** and the **1**-SiO<sub>2</sub> hybrid.

remained on the silica, showing that the hybrid obtained in the solvent-free system at a higher temperature is much more stable against hydrolysis.

The DSC traces of **1** and the **1**-SiO<sub>2</sub> hybrid are shown in Figure 5. **1** showed a melting point at 293 °C, while **1**-SiO<sub>2</sub> did not show any phase transition up to 400 °C. No phase transition of the **1**-silica hybrid demonstrated that **1** was attached to the surface of silica and was not able to move freely. Crystal to liquid transition of **1** at 293 °C was also confirmed by polarized optical microscopic observation.

**Reaction of 1 with Silicate Glass in Pyridine.** A similar procedure was applied to the functionalization of silicate glass with **1**. To a pyridine solution of **1** was placed a silicate glass, and the pyridine was heated at 110 °C to evaporate the solvent over a period of 1 h. When the solvent was evaporated, a portion of pyridine was added and the solution was heated again at 110 °C. Evaporation and pyridine addition was repeated three times. The resulting glass was rinsed with pyridine thoroughly. Adsorption of **1** could not be detected by using UV-visible spectroscopy but was confirmed by using the fluorescence emission spectrum as shown in Figure S1 (Supporting Information). The chloroform solution of **1** showed fluorescence emission maxima at 658 and 718 nm, while the silicate glass treated with **1** showed those at 653 and 709 nm.

**Reaction of 1 with Silicate Glass Using a Solid-Solid Reaction.** We attempted to perform the reaction in a solvent-free system: a spin-coated film of **1** on silicate glass was heated at various temperatures. The heat-treated glass was sonicated in pyridine to remove unreacted **1**. The resulting silicate glass was then analyzed with UV-visible spectroscopy.

In Figure 6, the UV-visible spectra of the glass after heat treatment at 80–250 °C for 10 min followed by sonication in pyridine to remove unreacted **1** are shown. The values of  $\lambda_{\max}$ , absorbance at  $\lambda_{\max}$ , and the surface coverage calculated by the equation shown in the table footnote are listed in Table 3. The absorbance of the Soret band increases with heating temperature. In the glass heated at 80 °C, the Soret band could hardly be detected. The absorption maximum of **1** in pyridine was 426 nm and the absorption maximum of the glass heated at 130 °C was 421 nm. On the other hand, the absorption maximum of the glass heated above 190 °C was red-shifted to 433–437 nm, with increasing the absorbance in the Soret band. These observations imply that the molecules **1** on the

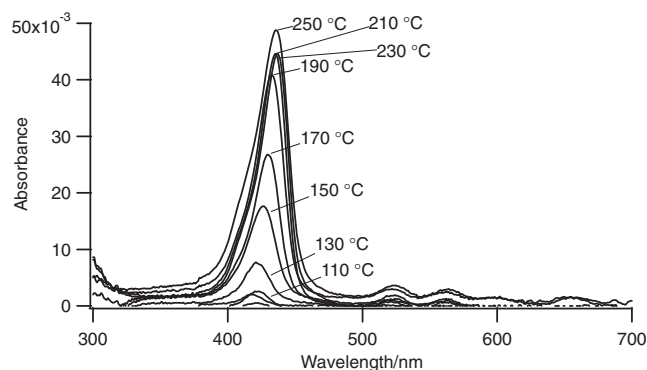


**Figure 6.** UV-visible spectra of porphyrin alcohol **1** spin-coated on silicate glass followed by heat treatment at 80, 90, 100, 110, 130, 150, 170, 190, 210, 230, and 250 °C for 10 min. The absorption maximum at 130 °C was 421 nm while that at 250 °C was 436 nm.

**Table 3.** UV-visible Spectra of **1** on Silicate Glass<sup>a)</sup>

Temperature /°C	$\lambda_{\max}$ /nm	Absorbance at $\lambda_{\max}$	Number of porphyrin molecules per 100 nm <sup>2</sup>
80	—	—	—
90	418	0.002	2
110	421	0.003	3
130	421	0.008	9
150	426	0.018	20
170	430	0.027	30
190	433	0.041	46
210	435	0.045	50
230	437	0.045	50
250	436	0.049	55
296	436	0.103	115

a)  $\lambda_{\max} = 426$  nm,  $\epsilon_{\max} = 5.38 \times 10^5$  cm<sup>-1</sup> M<sup>-1</sup> in pyridine. Number of porphyrin molecules per 100 nm<sup>2</sup> =  $AN_A/\epsilon_{\max} \times 10^{15}$  where  $N_A$  is the Avogadro number, and  $A$  is the absorbance at  $\lambda_{\max}$ .<sup>41</sup>

glass plate formed under the conditions of heating temperatures of 90–130 °C possibly exist as an isolated molecule, while those of heating temperatures above 190 °C form aggregates on the glass surface. The red shift also suggests that the porphyrin molecules form a head to tail aggregate, i.e., a J-type aggregate.<sup>42</sup> The temperatures at which the reaction occurs are well below the melting point of **1** (293 °C), indicating that the reaction occurs between the two solid phases.

The kinetics of the solid–solid reaction of **1** with silicate glass at 100–170 °C is shown in Figure 7. The reaction was slow at 100 °C, while saturation was observed above 130 °C, and the absorbance at saturation was 0.045 regardless of the reaction temperatures. The plot of the absorbance against time can be fit using Langmuir rate equation:  $-\ln(1 - A(t)/A(\infty)) = kt$ , where  $A(t)$ ,  $A(\infty)$ ,  $k$ , and  $t$  are absorbance at time  $t$ , absorbance after the reaction was complete, the rate constant, and the heating period, respectively. The rate constants  $k$  were 0.0008 min<sup>-1</sup> at 100 °C, 0.0106 min<sup>-1</sup> at 130 °C, 0.0274 min<sup>-1</sup> at 150 °C, and 0.104 min<sup>-1</sup> at 170 °C. The Arrhenius plot of  $\ln k$  vs.  $1/T$  gave the activation energy of 93 kJ mol<sup>-1</sup> for the reaction.

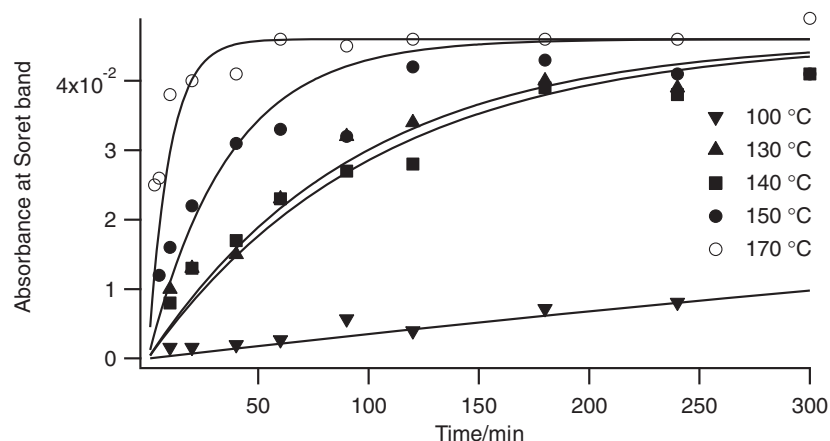


**Figure 7.** Plot of absorbance of the absorption maxima of the Soret band at 423–436 nm of a silicate glass spin-coated with **1** and heated at 100, 130, 140, 150, and 170 °C against heating periods. The curve obtained by fit the data to Langmuir adsorption rate equation:  $Abs = 0.046(1 - \exp(-kt))$  is shown, where  $k = 0.0008$  (100 °C), 0.0106 (130 °C), 0.0097 (140 °C), 0.0274 (150 °C), and 0.104  $\text{min}^{-1}$  (170 °C).

**Aggregate Structure Deduced from Kasha's Exciton Coupling Theory.** According to the Kasha's exciton coupling theory, the spectral shift observed for a dimer with a distinct geometry can be calculated using the equation:

$$\Delta E = \frac{\mu^2(1 - 3 \cos^2 \theta)}{4\pi\epsilon_0 r^3} \quad (1)$$

where  $\mu$  is the transition dipole moment,  $\theta$  is the angle between the two transition dipoles,  $\epsilon_0$  is the permittivity in vacuo, and  $r$  is the distance between the two chromophores. Putting all the physical constants in the above equation, we obtain the following equation:

$$\Delta E/\text{J mol}^{-1} = 5.17 \times 10^{26}(\mu/D)^2(1 - 3 \cos^2 \theta)/(r/\text{m})^3 \quad (2)$$

The shift of 15 nm corresponds to the exciton coupling energy  $\Delta E$  of 10  $\text{kJ mol}^{-1}$ . According to the above equation,  $r$  can be calculated to be 0.9 nm assuming that the transition moment  $\mu = 8\text{D}$  and the angle  $\theta = 0$ . Figure 8 shows schematically the aggregate structure **1** on the silicate glass, where the porphyrin molecule is represented by a square.

**Stability of **1** Bound to Silicate Glass in Various Organic Solvents.** The porphyrin layer on silicate glass was immersed in various organic solvents at 25 °C for 5 h, and the decrease in absorbance of the Soret band was determined after washing with pyridine. The amounts of **1** immobilized on silicate glass after 5 h were 87%, 88%, 88%, 98%, 81%, 96%, 92%, and 86% in toluene, chloroform, THF, pyridine, DMF, DMSO, acetone, and methanol, respectively (Figure 9). Therefore the porphyrin layer is rather stable in broad ranges of organic solvents. The porphyrin–silicate glass hybrid can be subjected to further chemical reactions, and such reactions will be reported elsewhere.

**Reaction of Ester Porphyrin and Ether Porphyrin with Silicate Glass.** In order to determine the role of the hydroxy groups of **1** in the reaction with silicate glass, we performed similar experiments using reference porphyrins, ester porphyrin, 5,10,15,20-tetrakis[4-(5-acetoxypentyloxy)phenyl]porphyrin (**2**), and ether porphyrin, 5,10,15,20-tetrakis(4-hexyloxyphenyl)porphyrin (**3**). The UV–visible spectra of a spin-coated

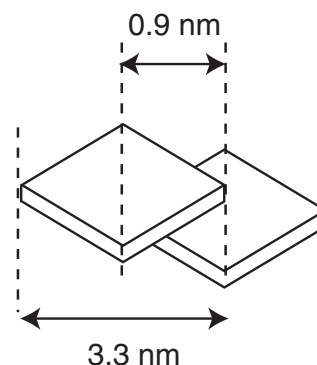


**Figure 8.** Schematic representation of a dimer structure deduced from the UV–visible spectral shift for an aggregate of **1**. The molecule of **1** is shown as a square. The distance between the centers of **1** was calculated to be 0.9 nm on the basis of Kasha's theory.

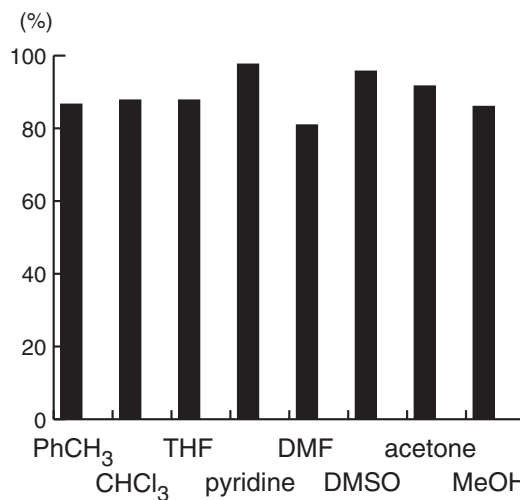


**Figure 9.** Absorbance of the Soret band of **1** on silicate glass after immersion in various organic solvents for 5 h at 25 °C and washing with pyridine.

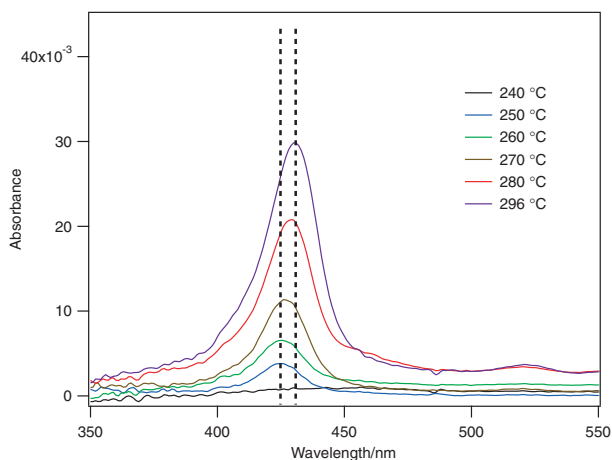


**Figure 10.** UV-visible spectra of ether porphyrin **3** spin-coated on silicate glass followed by heat treatment at the designated temperatures between 240 and 296 °C for 10 min. The absorption maximum heated at 296 °C was 430 nm while that heated at 250 °C was 426 nm.

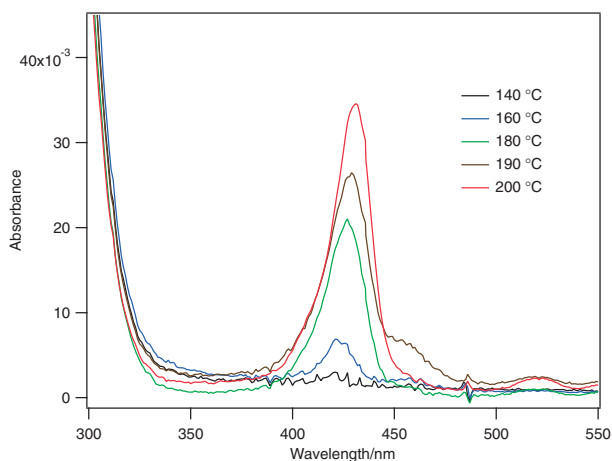


**Figure 11.** UV-visible spectra of ester porphyrin **2** spin-coated on silicate glass followed by heat treatment at the designated temperatures between 140 and 200 °C for 10 min. The absorption maximum heated at 200 °C was 431 nm while that heated at 160 °C was 421 nm.

film on silicate glass after heat treatment and sonication in pyridine are shown in Figures 10 and 11.

When the spin-coated film of ether porphyrin **3** was heated below 240 °C, no absorption of the Soret band was detected. The porphyrin was detected when the heating temperature was raised to 250 °C, and the absorbance of the Soret band increased as the temperature was raised further. A red shift from 426 to 430 nm was also observed as the temperature was higher. The values of  $\lambda_{\max}$ , absorbance, and the surface coverage are listed in Table 4. The sluggish reaction of the ether porphyrin **3** with silicate glass demonstrated that the hydroxy groups in **1** played an important role in the reaction with SiO<sub>2</sub>.

Figure 11 shows the UV-visible spectra of ester porphyrin **2**, which has acetate groups at the termini, spin-coated on the glass, heated at 140–200 °C, and sonicated in pyridine. Table 5 summarizes the spectral data of **2** adsorbed on silicate glass.

**Table 4.** UV-visible Spectra of **3** on Silicate Glass<sup>a)</sup>

Temperature / °C	$\lambda_{\max}$ / nm	Absorbance at $\lambda_{\max}$	Number of porphyrin molecules per 100 nm <sup>2</sup>
240	—	—	—
250	426	0.003	5
260	426	0.006	10
270	426	0.011	17
280	430	0.020	32
296	430	0.029	46

a)  $\lambda_{\max} = 425$  nm,  $\epsilon_{\max} = 3.79 \times 10^5$  cm<sup>-1</sup> M<sup>-1</sup> in pyridine.

**Table 5.** UV-visible Spectra of **2** on Silicate Glass<sup>a)</sup>

Temperature / °C	$\lambda_{\max}$ / nm	Absorbance at $\lambda_{\max}$	Number of porphyrin molecules per 100 nm <sup>2</sup>
140	—	—	—
160	426	0.006	7
180	427	0.021	26
190	429	0.026	32
200	431	0.035	44

a)  $\lambda_{\max} = 425$  nm,  $\epsilon_{\max} = 4.84 \times 10^5$  cm<sup>-1</sup> M<sup>-1</sup> in pyridine.

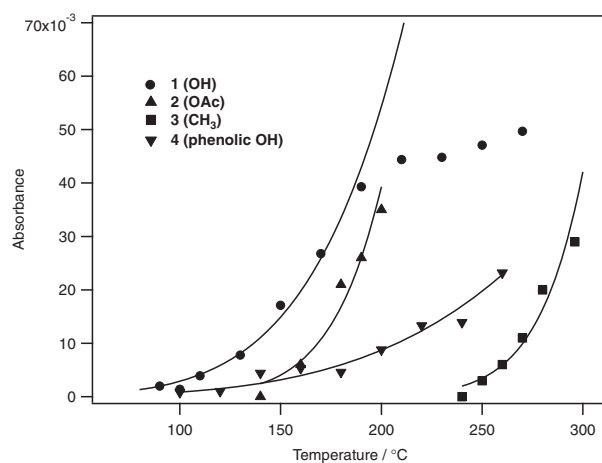


**Figure 12.** Plot of absorbance of the Soret band against the reaction temperatures for **1**, **2**, **3**, and **4**. The reaction period was 10 min. The curves fit to the Arrhenius equation,  $Abs = A \exp(-\Delta E / (temp + 273.15))$ , are shown. The absorbance of **1** heat-treated above 210 °C was much lower than expected from the Arrhenius equation.

The reaction of **2** with silicate glass proceeded when the temperature was above 160 °C. The melting point of **2** was 198 °C. Thus, the reaction of **2** with silicate glass proceeded across the solid–solid interface. Porphyrin **1** having OH groups reacted with silicate glass at a lower temperature than did **2** having OAc groups. Figure 12 shows the plot of absorbance of the Soret band of the porphyrins after reaction with silicate glass against the reaction temperatures. Four porphyrins reacted with silicate glass at different temperatures: the reactivity decreases in the order **1** (OH) > **2** (OAc) > **4** (phenolic OH)  $\gg$  **3** (CH<sub>3</sub>). The reaction of **1** with silicate glass could be initiated by a nucleophilic attack of the oxygen atom of alcohol of **1** on the Si atom, while the reaction of **2** may proceed via the acetyl transfer from **2** to SiOH followed by the nucleophilic attack of

the alcohol oxygen on the Si atom. The lower reactivity of **2** suggests that an acetate group can be used as a protecting group in the functionalization of silicate glass.

### Conclusion

Tetrahydroxyphyrin was allowed to react with silica gel and silicate glass either by use of pyridine as a solvent or by use of a solid–solid reaction. In the reaction in pyridine, removal of water from the reaction mixture by evaporating solvents assisted the adsorption reaction. Tetrahydroxyphyrin was allowed to react with silicate glass below the melting point, i.e., in a solid–solid reaction. A spin-coated film of the porphyrin was heated at 90–250 °C to yield a glass modified with the porphyrins. The amounts of porphyrins adsorbed increased with increasing temperature and the reaction periods, and showed saturation, displaying that monolayer film of porphyrin formed. As the coverages of porphyrin increased, the Soret band was shifted from 421 to 436 nm, suggesting that the porphyrin was adsorbed as a J-type aggregate. The reaction of tetraalkoxyphyrin with silicate glass occurred at much higher temperature around 250 °C, and the reaction of tetraacetoxyporphyrin at 160 °C. The different reactivities of the ether, ester, and alcohol functional groups can be useful for multiple functionalization of silica with organic molecules.

We thank Tokyo Ohka Foundation for the Promotion of Science and Technology for support of this research. This work was also supported by “Creating Research Center for Advanced Molecular Biochemistry,” Strategic Development of Research Infrastructure for Private Universities, the Ministry of Education, Culture, Sports, Science and Technology (MEXT), Japan.

### Supporting Information

Synthesis of porphyrin derivatives, **1**, **2**, and **3**; calculation of amounts of adsorbed porphyrin on silica gel based on TG traces, and fluorescence spectra of **1** adsorbed on silicate glass (PDF). This material is available free of charge via the web at <http://www.csj.jp/journals/bcsj/>.

### References

- 1 A. Vilan, A. Shanzer, D. Cahen, *Nature* **2000**, *404*, 166.
- 2 M. A. Rampi, G. M. Whitesides, *Chem. Phys.* **2002**, *281*, 373.
- 3 J. C. Scott, L. D. Bozano, *Adv. Mater.* **2007**, *19*, 1452.
- 4 E. Matsui, N. N. Matsuzawa, O. Harnack, T. Yamauchi, T. Hatazawa, A. Yasuda, T. Mizutani, *Adv. Mater.* **2006**, *18*, 2523.
- 5 A. G. MacDiarmid, *Angew. Chem., Int. Ed.* **2001**, *40*, 2581.
- 6 F. Louwet, L. Groenendaal, J. Dhaen, J. Manca, J. Van Luppen, E. Verdonck, L. Leenders, *Synth. Met.* **2003**, *135–136*, 115.
- 7 L. Groenendaal, F. Jonas, D. Freitag, H. Pielartzik, J. R. Reynolds, *Adv. Mater.* **2000**, *12*, 481.
- 8 M. Grundner, H. Jacob, *Appl. Phys. A: Mater. Sci. Process.* **1986**, *39*, 73.
- 9 H. Ibach, H. D. Bruchmann, H. Wagner, *Appl. Phys. A: Mater. Sci. Process.* **1982**, *29*, 113.
- 10 S. I. Raider, R. Flitsch, M. J. Palmer, *J. Electrochem. Soc.* **1975**, *122*, 413.
- 11 R. J. Archer, *J. Electrochem. Soc.* **1957**, *104*, 619.
- 12 B. Ulgut, S. Suzer, *J. Phys. Chem. B* **2003**, *107*, 2939.
- 13 A. H. Carim, M. M. Dovek, C. F. Quate, R. Sinclair, C. Vorst, *Science* **1987**, *237*, 630.
- 14 H. Ishii, S. Hasegawa, D. Yoshimura, K. Sugiyama, S. Narioka, M. Sei, Y. Ouchi, K. Seki, Y. Harima, K. Yamashita, *Mol. Cryst. Liq. Cryst.* **1997**, *296*, 427.
- 15 H. Ishii, K. Sugiyama, E. Ito, K. Seki, *Adv. Mater.* **1999**, *11*, 605.
- 16 E. Tran, M. Duati, V. Ferri, K. Müllen, M. Zhamikov, G. M. Whitesides, M. A. Rampi, *Adv. Mater.* **2006**, *18*, 1323.
- 17 L. Wei, D. Syomin, R. S. Loewe, J. S. Lindsey, F. Zaera, D. F. Bocian, *J. Phys. Chem. B* **2005**, *109*, 6323.
- 18 Z. Liu, A. A. Yasseri, J. S. Lindsey, D. F. Bocian, *Science* **2003**, *302*, 1543.
- 19 K. M. Roth, A. A. Yasseri, Z. Liu, R. B. Dabke, V. Malinovskii, K.-H. Schweikart, L. Yu, H. Tiznado, F. Zaera, J. S. Lindsey, W. G. Kuhr, D. F. Bocian, *J. Am. Chem. Soc.* **2003**, *125*, 505.
- 20 C. Liu, J. B. Lambert, L. Fu, *J. Org. Chem.* **2004**, *69*, 2213.
- 21 J. H. Song, M. J. Sailor, *Comments Inorg. Chem.* **1999**, *21*, 69.
- 22 N. Y. Kim, P. E. Laibinis, *J. Am. Chem. Soc.* **1997**, *119*, 2297.
- 23 X.-Y. Zhu, V. Boiadjev, J. A. Mulder, R. P. Hsung, R. C. Major, *Langmuir* **2000**, *16*, 6766.
- 24 R. Boukherroub, S. Morin, P. Sharpe, D. D. M. Wayner, P. Allongue, *Langmuir* **2000**, *16*, 7429.
- 25 J. E. Bateman, R. D. Eagling, B. R. Horrocks, A. Houlton, *J. Phys. Chem. B* **2000**, *104*, 5557.
- 26 H. Dislich, *Angew. Chem., Int. Ed. Engl.* **1971**, *10*, 363.
- 27 K. S. Mazdiyasi, R. T. Dolloff, J. S. Smith, *J. Am. Ceram. Soc.* **1969**, *52*, 523.
- 28 For reviews of functionalization reactions of inorganic surfaces, see: Z. Ma, F. Zaera, *Surf. Sci. Rep.* **2006**, *61*, 229.
- 29 B. J. Vesper, K. Salaita, H. Zong, C. A. Mirkin, A. G. M. Barrett, B. M. Hoffman, *J. Am. Chem. Soc.* **2004**, *126*, 16653.
- 30 A. Gulino, P. Mineo, I. Fragalà, *J. Phys. Chem. C* **2007**, *111*, 1373.
- 31 A. Gulino, S. Bazzano, P. Mineo, E. Scamporrino, D. Vitalini, I. Fragalà, *Chem. Mater.* **2005**, *17*, 521.
- 32 O. M. Dzhigit, A. V. Kiselev, N. N. Mikos-Avgul, K. D. Shcherbakova, *Dokl. Akad. Nauk SSSR* **1950**, *70*, 441.
- 33 T. Mizutani, K. Takahashi, T. Kato, J. Yamamoto, N. Ueda, R. Nakashima, *Bull. Chem. Soc. Jpn.* **1993**, *66*, 3802.
- 34 C. C. Ballard, E. C. Broge, R. K. Iler, D. S. S. John, J. R. McWhorter, *J. Phys. Chem.* **1961**, *65*, 20.
- 35 S. Shioji, M. Kawaguchi, Y. Hayashi, K. Tokami, H. Yamamoto, *Adv. Powder Technol.* **2001**, *12*, 343.
- 36 H. Utsugi, H. Horikoshi, T. Matsuzawa, *J. Colloid Interface Sci.* **1975**, *50*, 154.
- 37 T. Kimura, K. Kuroda, Y. Sugahara, K. Kuroda, *J. Porous Mater.* **1998**, *5*, 127.
- 38 G. C. Ossenkamp, T. Kemmitt, J. H. Johnston, *Chem. Mater.* **2001**, *13*, 3975.
- 39 P. Battioni, E. Cardin, M. Louloui, B. Schöllhorn, G. A. Spyroulias, D. Mansuy, T. G. Traylor, *Chem. Commun.* **1996**, 2037.
- 40 G. C. Ossenkamp, T. Kemmitt, J. H. Johnston, *Langmuir* **2002**, *18*, 5749.
- 41 D. Q. Li, B. I. Swanson, J. M. Robinson, M. A. Hoffbauer, *J. Am. Chem. Soc.* **1993**, *115*, 6975.
- 42 M. Kasha, *Radiat. Res.* **1963**, *20*, 55.